Talanta 129 (2014) 72–78

Contents lists available at ScienceDirect

Talanta

journal homepage: www.elsevier.com/locate/talanta

A miniaturized capacitively coupled plasma microtorch optical emission spectrometer and a Rh coiled-filament as small-sized electrothermal vaporization device for simultaneous determination of volatile elements from liquid microsamples: Spectral and analytical characterization

Tiberiu Frentiu [a,*], Eugen Darvasi [a], Sinziana Butaciu [a], Michaela Ponta [a], Dorin Petreus [b], Alin I. Mihaltan [c], Maria Frentiu [c]

[a] Babes-Bolyai University, Faculty of Chemistry and Chemical Engineering, Arany Janos 11, 400028 Cluj-Napoca, Romania
[b] Technical University of Cluj-Napoca, Faculty of Electronics, Telecommunications and Information Technology, Gh. Baritiu 26-28, 400027 Cluj-Napoca, Romania
[c] INCDO-INOE 2000 National Institute for Research and Development of Optoelectronics Bucharest, Research Institute for Analytical Instrumentation, Donath 67, 400293 Cluj-Napoca, Romania

ARTICLE INFO

Article history:
Received 12 February 2014
Received in revised form
9 April 2014
Accepted 15 April 2014
Available online 15 May 2014

Keywords:
Capacitively coupled plasma microtorch
Electrothermal vaporization
Rh-coiled filament
Microspectrometer
Optical emission spectrometry
Multielemental analysis

ABSTRACT

A low power and low argon consumption (13.56 MHz, 15 W, 150 ml min^{-1}) capacitively coupled plasma microtorch interfaced with a low-resolution microspectrometer and a small-sized electrothermal vaporization Rh coiled-filament as liquid microsample introduction device into the plasma was investigated for the simultaneous determination of several volatile elements of interest for environment. Constructive details, spectral and analytical characteristics, and optimum operating conditions of the laboratory equipment for the simultaneous determination of Ag, Cd, Cu, Pb and Zn requiring low vaporization power are provided. The method involves drying of 10 µl sample at 100 °C, vaporization at 1500 °C and emission measurement by capture of 20 successive spectral episodes each at an integration time of 500 ms. Experiments showed that emission of elements and plasma background were disturbed by the presence of complex matrix and hot Ar flow transporting the microsample into plasma. The emission spectrum of elements is simple, dominated by the resonance lines. The analytical system provided detection limits in the ng ml^{-1} range: 0.5(Ag); 1.5(Cd); 5.6 (Cu); 20(Pb) and 3(Zn) and absolute detection limits of the order of pg: 5(Ag); 15(Cd); 56(Cu); 200(Pb) and 30 (Zn). It was demonstrated the utility and capability of the miniaturized analytical system in the simultaneous determination of elements in soil and water sediment using the standard addition method to compensate for the non-spectral effects of alkali and earth alkaline elements. The analysis of eight certified reference materials exhibited reliable results with recovery in the range of 95–108% and precision of 0.5–9.0% for the five examined elements. The proposed miniaturized analytical system is attractive due to the simple construction of the electrothermal vaporization device and microtorch, low costs associated to plasma generation, high analytical sensitivity and easy-to-run for simultaneous multielemental analysis of liquid microsamples.

1. Introduction

In the last decade microplasmas, also known as microdischarges, embedded in benchtop-sized or portable analytical instrumentation, characterized by low power in-put, low Ar or He consumption and simple emission spectrum of analytes received increased attention as viable alternative to conventional laboratory systems based on inductively coupled plasma atomic spectrometry [1–4]. Their applications referred mainly to determination of Hg in gaseous or liquid samples after cold vapor generation, As and Sb after hydride derivatization [5–14] and detection in gas chromatography [15]. Liquid electrode plasmas sustained in contact with a small-sized flowing/non-flowing liquid cathode were reported as useful multielemental detectors in the analysis of microsamples introduced into plasma by cathode sputtering [16–18]. It has been demonstrated in our laboratory that an argon capacitively coupled plasma microtorch (µCCP) (13.56 MHz, 30 W) is satisfactory for elemental analysis by optical emission spectrometry (OES) of liquid samples pneumatically/ultrasonically nebulized without/with desolvation [19,20].

* Corresponding author. Tel.: +40 264 593833; fax.: +40 264 590818.
E-mail address: ftibi@chem.ubbcluj.ro (T. Frentiu).

http://dx.doi.org/10.1016/j.talanta.2014.04.032
0039-9140/

Forty years ago Williams and Piepmeier [21] reported on the electrothermal vaporization (ETV) from a W filament coil as introduction device of liquid microsamples. The use of W coiled-filament resulted in the improvement of analytical detection capability of spectrometric techniques such as atomic absorption (ETV–AAS), optical emission/mass spectrometry in inductively coupled plasma (ETV-ICP-OES/MS) and atomic fluorescence (ETV–AFS) especially for volatile and medium volatile elements (Cd, Pb, Hg and As) [22]. The preconcentration of hydride forming elements on a W coil coated or not with an inert element with catalytic property (Ir, Rh, Au, Pt) resulted in an improvement of 20–200 times of the detection limits [23–25].

Badiei et al. [26–28] reported a 40-fold improvement of the detection limits for Pb and Cr in sea and tap water by electrothermal near-torch vaporization inductively coupled plasma optical emission spectrometry (NTV–ICP-OES). The method involved on-site collection of liquid microsamples or concentration by electrodeposition of metallic species on a portable Re coiled-filament, sample drying and analysis in laboratory. The ETV approach opens the door to the use of microplasmas in the simultaneous multielemental analysis of liquid microsamples. Thus, Karanassios et al. [29] and Weagant et al. [30,31] demonstrated the analytical utility of a battery-operated He/Ar–H_2 atmospheric-pressure microplasma in optical emission spectrometry (ETV–MPD-OES) for simultaneous determination of low volatile/excitable elements with absolute detection limits in the nanogram or even picogram range.

This paper presents the spectral and analytical evaluation of a miniaturized laboratory system based on small-sized electrothermal vaporization device and detection by capacitively coupled plasma microtorch optical emission spectrometry (SSETV–μCCP-OES) in the simultaneous determination of several volatile elements (Ag, Cd, Cu, Pb and Zn) from liquid microsamples. The elements were selected because of their significance for environment. Constructive details of the analytical system and a characterization in terms of spectral response, detection limit, precision and accuracy of determinations, and non-spectral interference from alkali and earth-alkaline elements on analytes emission are given. The influence of the temperature program of the electrothermal vaporization and plasma microtorch operation on analytical performance was studied to optimize the simultaneous determination of the tested elements. The strengths and weaknesses of the new concept compared with other analytical systems are presented. Analytical applicability and utility of the innovative SSETV–μCCP-OES system were demonstrated for the simultaneous determination of the tested elements in several certified reference materials of soil and sediment.

2. Experimental

2.1. Instrumentation

The SSETV–μCCP-OES experimental equipment consists of a small-sized electrothermal vaporization device, a HM 7042-5 triple power supply unit, a μCCP supplied from a miniaturized free-running RF generator and a QE65 Pro microspectrometer. The schematic of the SSETV–μCCP-OES set-up is given in Fig. 1, μCCP and electrothermal device in Fig. 2(a) and (b) as well as in Supplementary material 1. The prefix micro before the terms electrode, plasma, torch and entire set-up, which refers in *stricto sensu* to devices having at least one dimension less that 100 μm, was used since the definition has been relaxed to include millimeter-size devices [1].

The SSETV device (Home-made, Babes-Bolyai University, Cluj-Napoca, Romania) consists of a T-shaped vaporization chamber of

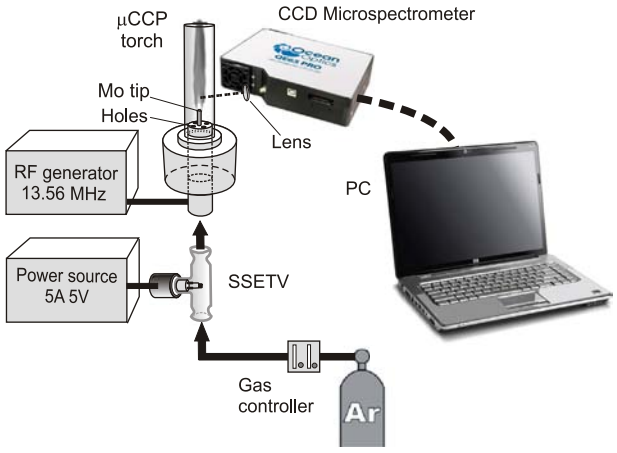

Fig. 1. Schematic of the SSETV-μCCP-OES set-up.

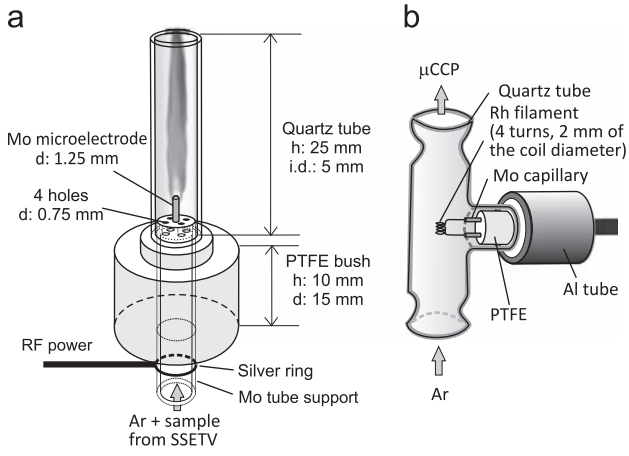

Fig. 2. (a) Capacitively coupled plasma microtorch; and (b) Rh small-sized electrothermal vaporization device.

2.5 cm^3 made of a quartz tube with 8 mm i.d. and 10 mm o.d. Inside the tube there is a 0.25 mm thick coil-filament (4 turns) of Rh, 99.9% purity temper annealed (Goodfellow, Cambridge, UK). The linear ends of the coil filament come out from the vaporization chamber through two Mo capillaries of 0.7 mm i.d. and 1 mm o.d. crossing a PTFE holder fixed in one of the arms of the T-shaped vaporization chamber. The electrical power from the HM 7042-5 supply unit (Hameg Instruments, Mainhausen, Germany) is carried to the coil filament *via* transfer cables. The SSETV device is mounted on a plunger in a PTFE holder allowing back and forth movements (Supplementary material 1). The operation of the SSETV device involved filament heating in two steps, one designed to slowly dry the microsample and the other to achieve its rapid vaporization. Firstly, the Rh coiled-filament was retracted from the vaporization chamber by moving back the plunger in the holder (Supplementary material 1) and a volume of 10 μl sample was deposited onto the filament using a Hamilton pipette. Sample drying occurred in the air by heating the filament for 80 s at 0.55 W power level (0.26 V and 2.11 A). The Rh coil filament was then reinserted by pushing the plunger until the PTFE support reached the T-arm of the vaporization chamber and fit effortless inside. Subsequently, the microplasma was turned on and few seconds were necessary for background emission to stabilize. Further, the coil was supplied at 10.5 W (2.2 V and 4.77 A) for 6 s

and the vaporized sample was carried into plasma (Supplementary material 1) *via* 50–175 ml min^{-1} Ar flow rate.

Following the annealing of the Rh filament performed by the manufacturer, the filament became more ductile and more workable allowing the run of 2500–3000 heating and cooling cycles without becoming brittle. In the same time, the volatile impurities (Cd, Zn) were boiled-off, while the other elements mentioned in the sheet product at the level of 1 μg g^{-1} Ag and Pb and 20 μg g^{-1} Cu had no influence on the detection limit of these elements in soil and sediment samples. Beside the mechanical characteristics, other reasons were taken into account in the selection of the material for the coil filament. Thus, Rh (1964 °C m.p.) is a chemically inert transition metal, completely insoluble in nitric acid and slightly soluble in aqua regia, does not retain oxygen at temperatures below its melting point and does not normally form oxides. These features are particularly important as the liquid samples subjected to analysis often result from acidic mineralization. Due to the exceptional corrosion resistance of Rh it is not necessary to create a hydrogen reducing atmosphere in the vaporization chamber, which would cause an increase of the background signal of Ar plasma in the UV range [13].

The μCCP torch (Home-made, INCDO-INOE 2000 Bucharest, Research Institute for Analytical Instrumentation, Cluj-Napoca, Romania) served to develop a 13.56 MHz RF plasma of low power (9–20 W) and low Ar consumption (50–175 ml min^{-1}) at the tip of a Mo microelectrode (1.25 mm diameter, Goodfellow, Cambridge, UK) mounted inside a quartz tube (5 mm i.d., 25 mm length, 160 nm cut-off; H. Baumbach & Co Ltd., Ipswich Suffolk, UK). A single Ar flow was used as plasma gas and for the introduction of electrothermal vaporized sample. The intake of Ar into plasma occurred through four 0.75 mm-diameter holes across the microelectrode support on a 3 mm-diameter rim. Plasma was generated as a diffuse bluish discharge (Supplementary material 1) at the tip of the microelectrode connected to a miniaturized free-running RF generator of 17 × 15 × 24 cm^3 (Technical University of Cluj-Napoca, Romania). The emission signal was registered over the spectral range 190–380 nm using the QE65 Pro microspectrometer (Ocean Optics, Dunedin, USA) interfaced to Laptop through the USB port and mounted on a XYZ translator to target different observation heights in plasma by 100 μm increment. The microspectrometer was equipped with a back-illuminated TE Cooled (−20 °C) Hamamatsu Detector, which allowed the decrease of the background emission to half as compared to the running without detector cooling. The emission signal was collected with no fiber optic, using a collector lens (10 mm focal distance) mounted in the front of the spectrometer slit (Supplementary material 1). The High Speed Acquisition mode of the Spectrasuite software was started simultaneously with sample vaporization to record 20 three-dimensional raw successive spectral episodes (intensity vs. wavelength vs. time) each with 500 ms integration time. The total net emission spectrum of analytes resulted from the summation of all 20 spectral episodes after background correction. The microtorch was not disconnected from the power supply and plasma was not turned off/on during sample drying/vaporization cycles. In this way the recorded spectra exhibited good repeatability, while the variance of the analytical signals in multiple measurements of the same standard or sample was at the 9% level or better.

2.2. Reagents, stock solutions and CRMs

Monoelemental standard solutions of 1000 μg ml^{-1} (Merck, Darmstadt, Germany) were used to prepare the necessary solutions within the study. Multielemental solutions containing 50 ng ml^{-1} Ag, Cd and Zn, 200 ng ml^{-1} Cu and 500 ng ml^{-1} Pb were used for the optimization of Rh-coil electrothermal vaporization program of sample and conditions for spectral episodes recording. The non-spectral interference of alkali and earth-alkaline elements was evaluated from the emission response of Ag, Cd, Cu, Pb and Zn in solution with the above mentioned concentrations in the presence of 0.01–100 μg ml^{-1} Li, Na, K, Ca and Mg as concomitants. Six reference materials of soil (RTC-CRM-048-50G Trace Metals Sand 1, RTC-CRM-025-050 Soil Sandy loam-Metals, LGC6135 Soil-Hackney Brick Works, LGC6141 Soil contaminated with clinker ash, CRM Soil Material S1 and BCR142R-Light Sandy Soil) and two of sediments (BCR-280R Lake sediment and NCS DC78301 River Sediment) from LGC Promochem, Wesel, Germany, were analyzed to demonstrate the capability of the SSETV–μCCP-OES analytical system. Solutions of 30% ultrapure HCl and 65% ultrapure HNO_3 (Merck, Darmstadt, Germany) were used for sample digestion. All solutions were prepared using ultrapure water (18 MΩ cm^{-1}) obtained in laboratory (Millipore Corp., Bedford, USA).

2.3. Preparation and analysis of CRMs

Amounts of 1.0000 g sample were subjected to digestion with 12 ml *aqua regia* in the PTFE vessels of the Berghof MWS3+microwave digester following a 4-step protocol previously presented [32]. After cooling, the digest was transferred into a 100 ml volumetric flask and diluted to the mark. Determination of Ag, Cd, Cu, Pb and Zn was carried out using the standard addition approach, commonly used to compensate for the non-spectral interferences of complex matrices.

To draw the calibration curve six aliquot volumes of 0.5–10 ml of digest were spiked with 0–2.5 ml solution containing 0.5 μg ml^{-1} Ag and Cd, and 5 μg ml^{-1} Cu, Pb and Zn, then diluted to 25 ml with water.

3. Results and discussion

3.1. Characteristics of the plasma background and emission spectrum of elements

The background spectrum emitted by the Ar μCCP is shown in Fig. 3(a), the background-subtracted episodic emission spectra of Ag, Cd, Cu, Pb and Zn and the total net spectrum are presented in Fig. 3(b) and (c).

The background spectrum in UV consists mainly of molecular emission from NO species ($X^2\Pi \rightarrow A^2\Sigma^+$, 205.28 (0,2), 215.49 (0,1), 223.61 (2,3), 226.94 (0,0), 237.02 (1,0), 247.87 (2,0), 259.60 (3.0)), OH ($X^2\Pi \rightarrow A^2\Sigma^+$, 282.90 (0,1), 308.90 (0,0)) and second positive system of N_2 ($C^3\Pi_u \rightarrow B^{\beta}_g$, 337.70 (0,0), 357.68 (0,1), 380.49 (0,2)).

As a consequence of the limited excitation capability of μCCP, similar to other low power microdischarges, emission spectrum of elements is simple, with few lines. As expected, the most prominent are the resonance lines with low excitation energy (< 7 eV). The low electron number density supports the idea of an overpopulation of low excitation energy levels of atoms [19]. Thus, the highest emission was measured for Cd at 228.802 nm (E_{ex} = 5.41 eV) and Zn at 213.856 nm (E_{ex} = 5.80 eV). In the case of Cu the observed lines were at 324.754 nm and 327.396 nm with E_{ex} = 3.82 eV, while for Ag at 328.068 nm (E_{ex} = 3.78 eV) and 338.289 nm (E_{ex} = 3.66 eV). Although in the case of Pb the 283.305 nm resonance line was the most intense, it exhibited spectral interference from OH molecular emission (282.90 nm), lower signal-to-background ratio (SBR), higher relative standard deviation of background (RSDB) and poorer detection limit as compared to the line at 368.346 nm (E_{ex} = 4.33 eV). Consequently, the latter was selected for Pb measurement. Although the spectral simplicity seems to be a limitation in terms of analytical lines

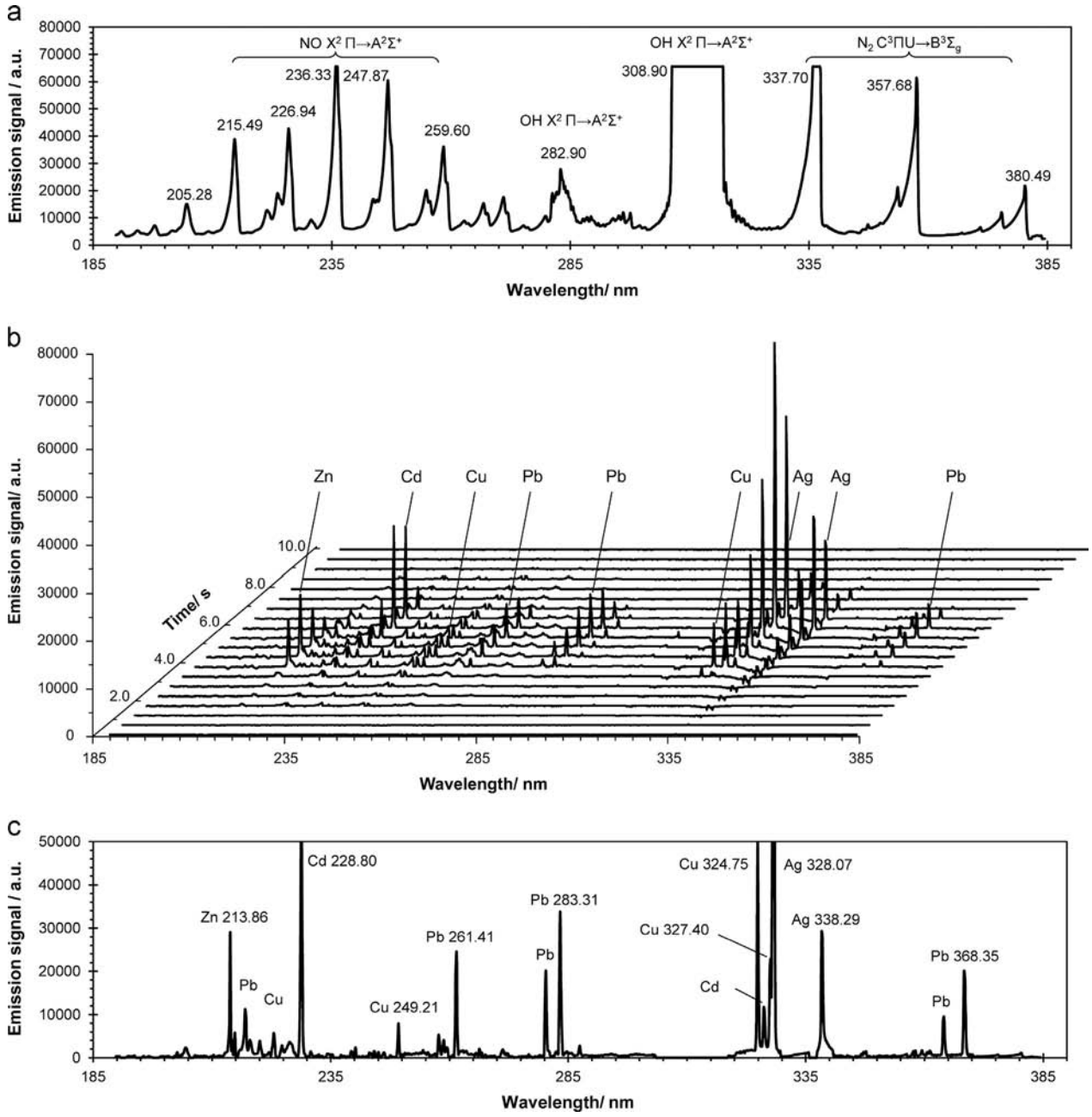

Fig. 3. (a) Background emission spectrum of the Ar μCCP; (b) Background-subtracted episodic emission spectra of elements in SSETV-μCCP-OES, (c) Total net emission spectrum of elements, measurement conditions: 10 μl sample volume containing 50 ng ml^{-1} Ag, Cd, Zn; 200 ng ml^{-1} Cu, 500 ng ml^{-1} Pb; drying temperature: 100 °C; electrothermal vaporization temperature: 1500 °C for 6 s; 15 W plasma power; 150 ml min^{-1} Ar flow rate as plasma gas; 0.8 mm observation height; 500 ms integration time per episode (20 episodes).

selection, it facilitates the use of a low resolution microspectrometer of 0.4 nm-FWHM.

3.2. Optimization of the working conditions of the SSETV–μCCP-OES system

The SSETV–μCCP-OES system was optimized in terms of temperature program of the electrothermal vaporization device and operating parameters of the plasma microtorch. The parameters under consideration to optimize the SSETV device were drying time and drying/vaporization temperature. The temperature was varied by modifying the coil power supply up to 11 W. The power absorbed by the coil was calculated as the product of the applied voltage and the corresponding measured current. The coil temperature in the range 20–700 °C was measured using a small-sized Pt-Au thermocouple (100 μm wires diameter, in-house calibrated), while in the range 700–1600 °C using an optical pyrometer (Siemens-Halske, Germany) in combination with a converging lens focalized on the filament. The correlation between the coil filament temperature and supplied voltage is shown in Supplementary material 2. This dependence shows that a careful adjustment of the absorbed power results in a precise control of the coil temperature up to 1600 °C (RSD < 5%). The curve served to establish a power level of 0.55 W (0.26 V; 2.11 A) to reach 100 °C for microsample drying. The time necessary to dry 10 μl sample was determined based on the current variation through the coil supplied at 0.26 V due to changing in resistivity during sample drying (Supplementary material 3). One can notice a sharp drop in

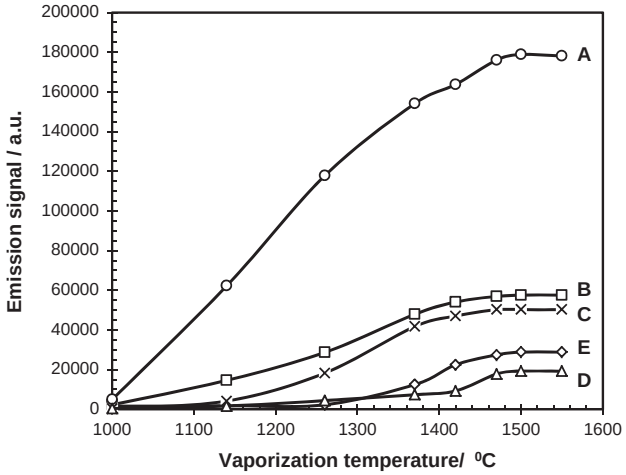

Fig. 4. Variation of total analyte emission as a function of vaporization temperature of sample from the Rh coil filament. A is Ag; B is Cd; C is Cu; D is Pb, E is Zn., measurement conditions: 10 μl sample volume containing 50 ng ml^{-1} Ag, Cd, Zn; 200 ng ml^{-1} Cu, 500 ng ml^{-1} Pb; drying temperature: 100 °C; 15 W plasma power; 150 ml min^{-1} Ar flow rate as plasma gas; 0.8 mm observation height.

current through the filament at the end of the drying step, so that a period of 80 s was considered as optimal for the drying of 10 μl sample at 100 °C.

The optimization of the vaporization temperature of the dried microsample was made for the highest spectral response of analytes. Emission measurements were performed by different power levels supplied to the coil filament corresponding to temperatures in the range 1000–1600 °C. The used analytical lines of the tested elements were Ag 328.068 nm, Cd 228.802 nm, Cu 324.754 nm, Pb 368.346 nm and Zn 213.856 nm. The effect of the coil temperature on the response is illustrated in Fig. 4.

The curve shapes indicate an increase of the emission signal with the vaporization temperature. Also, the increase of vaporization temperature resulted in fewer episodes containing signals from analytes, higher calibration sensitivity and larger dynamic range (Table 1).

The background-subtracted spectral episodes showed a selective thermal vaporization of elements, since emission signal of analytes appeared in different sequences. A 6 s heating time at a vaporization temperature of 1500 °C and capture of 20 successive episodes, each at an integration time of 500 ms, allowed the recording of total emission for Ag, Cd, Cu, Pb and Zn. Under such conditions the simultaneous determination of these elements was possible.

The operation of the plasma microtorch was optimized in terms of power supply, Ar flow rate and observation height to obtain the maximum emission signal of analytes and the highest signal-to-background ratio. The SBR was calculated by dividing the total net signal of analytes to the sum of the background signals from episodes containing the useful signal. For the elements under study, the optimal plasma conditions were 15 W and 150 ml min^{-1} Ar flow rate. The variation of SBR vs. observation height under the optimal conditions for a solution containing 50 ng ml^{-1} Ag, Cd, Zn, 200 ng ml^{-1} Cu and 500 ng ml^{-1} Pb is illustrated in Fig. 5.

The curves in Fig. 5 show no relationship between optimum observation height and excitation energy of analytes, which allows the simultaneous determination of Ag, Cd, Zn, Cu and Pb at 0.8 mm observation height in μCCP. The occurrence of the maximum emission of these elements at low observation height suggests the involvement of electrons emitted by the hot microelectrode both in plasma sustaining and excitation process of analyte atoms. Results are consistent with the sharp drop of the

Table 1
Effect of the vaporization temperature on dynamic range, calibration sensitivity and correlation coefficients in SSETV-μCCP-OES.

Element	Temperature (°C)	Dynamic range (μg ml^{-1})	Calibration sensitivity × 10^{-3} (peak height signal/ng ml^{-1})	Correlation coefficient
Ag	1250	0.01–5	2350	0.998
	1350	0.005–5	3120	0.999
	1500	0.002–2	3580	0.999
Cd	1250	0.01–5	575	0.994
	1350	0.01–5	760	0.998
	1500	0.005–5	1150	0.999
Cu	1250	0.05–5	95	0.997
	1350	0.02–10	210	0.998
	1500	0.02–10	250	0.999
Pb	1250	0.2–20	10	0.998
	1350	0.1–20	15	0.999
	1500	0.05–50	40	0.999
Zn	1250	0.05–5	45	0.994
	1350	0.02–5	250	0.996
	1500	0.01–10	575	0.999

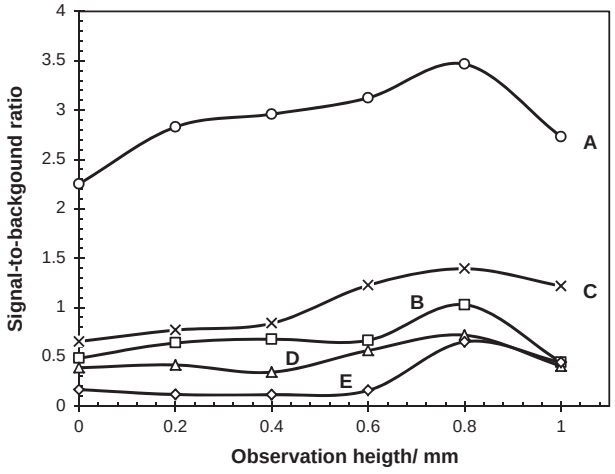

Fig. 5. Signal-to-background ratio vs. observation height for Ag (A), Cd (B), Cu (C), Pb (D), and Zn (E). Measurement conditions: 10 μl sample volume containing 50 ng ml^{-1} Ag, Cd, Zn; 200 ng ml^{-1} Cu, 500 ng ml^{-1} Pb; 15 W plasma power; 150 ml min^{-1} Ar flow rate.

excitation temperature over the range 0–1 mm heights above the microelectrode tip [19].

3.3. Non-spectral interferences of alkali and earth-alkaline elements

The non-spectral interferences of Li, Na, K, Ca and Mg up to 100 μg ml^{-1} concomitant on the emission of Ag, Cd, Cu, Pb and Zn are presented in Supplementary material 4. The non-spectral effect (EF) of a concomitant on the emission of an analyte was expressed as: $EF=(x^{m}_{net}-x^{0}_{net})\times 100/x^{0}_{net}$; where: x^{m}_{net}/x^{0}_{net} – net analyte emission signal in the presence/absence of matrix. A negative value of the EF stands for a depressive matrix effect, while a positive one for an enhancing effect. The plots in Supplementary material 4 show that the non-spectral effects are both matrix and analyte dependent. As a rule, the presence of Ca and Mg with low volatility and relatively high ionization energy resulted in enhancing matrix effects, while the easily ionizable elements (Na and K) of higher volatility induced a decrease of analyte emission. In short, Mg caused the greatest increasing effect, while Na the most depressive. It can be stated that the non-spectral effects occur in the gas phase in plasma rather than in solid phase during vaporization. The increasing matrix effect

caused by Mg and Ca could be explained by the involvement of electrons resulted from the concomitant ionization in the excitation mechanism of analytes. On the other hand, the depressive influence of alkali on analyte emission may be due to the increase in plasma size and thereby, lower power density. It can be remarked that the non-spectral effects of all tested matrices vary substantially up to a concentration of 20 μg ml^{-1} concomitant, after that a smoothing occurs. Overall, the low power plasmas are prone to matrix effect, which makes unsuitable the external calibration using aqueous standards. The phenomenon has been signaled by other authors using miniaturized discharges for elemental determinations in complex matrices [29–31].

3.4. Limits of detection

The limits of detection of elements were calculated based on the 3σ criterion and RSDB–SBR methodology [33], where RSDB was the relative standard deviation of the background and SBR the value obtained for a standard or sample solution falling within the dynamic range. In this study individual RSDB values were calculated for each episode from the signals measured in the vicinity of the analytical line using the same number of pixels (5) approximating the analytical line profile. Finally, an average RSDB of 0.8–1.3% was obtained from 20 individual values resulted from the successive two-dimensional spectra. This algorithm to calculate RSDB was imposed by the fact that plasma was disturbed by sample introduction resulting in changes of the background level during recording of the successive episodes (Supplementary material 5). The influence on the background was much greater in the case of soil samples with complex matrix than in the case of the synthetic multielemental aqueous standards.

The limits of detection calculated from measurements on synthetic solutions under the optimum working conditions together with those reported for other analytical methods are given in Table 2.

The detection limits of the tested elements in liquid samples by SSETV–μCCP-OES were in the range of ng ml^{-1}, between 0.5 (Ag)–20 (Pb), while the corresponding absolute values in the range of pg, namely 5 (Ag)–200 (Pb). Limits of detection are substantially better as compared to those found in μCCP-OES [19], CCP-OES [34] and CCP–AFS [32,35,36] with sample introduction as wet aerosol. The improvement is due to sample introduction as dry aerosol so that the dissipated power in plasma was used mostly for the dissociation of molecular species of analyte and excitation of the resulted atoms. The absolute detection limits in SSETV–μCCP-OES are better than in ETV–MPD-OES due to the 4-fold higher operating power in μCCP than in MPD, since spectral detectors are similar in the two approaches [31]. Measurements performed in μCCP at 9 W power level, close to that used in MPD, resulted in comparable detection limits in the two methods suggesting similar excitation capability. Although detection limits for some elements (Cu and Zn) are poorer in SSETV–μCCP-OES than in ICP-OES with pneumatic nebulization, the proposed equipment remains attractive in terms of construction and operation cost.

The detection limits expressed as dry mass for 1.0000 g soil sample mineralized to 100 ml solution were (mg kg^{-1}): 0.05 (Ag), 0.15 (Cd), 0.6 (Cu), 2 (Pb) and 0.3 (Zn), several times lower (7 for Cd, 10 for Pb, 33 for Cu, 40 for Ag and 300 Zn) than the normal values of these elements in soil, so that the SSETV–μCCP-OES method meets the requirement in terms of sensitivity for such determinations.

3.5. Chemical analysis

The results obtained in the multielemental analysis of several CRMs of soil and sediment using the standard addition approach to compensate for the non-spectral interferences are presented in Table 3. Three independently prepared and analyzed samples were considered for each CRM to calculate the mean concentration, recovery and expanded uncertainty for 95% confidence interval. The standard deviation of repeatability (precision) was determined from 5 successive measurements of each CRM.

Data in Table 3 demonstrate good agreement between found results and certified values with recovery in the range 95–108%. According to the t test there was no evidence of systematic error for 95% confidence level and $n=3$ replicates ($t_{tab}=4.303$). The overall standard deviation of repeatability for 5 successive measurements was in the range 0.5–9.0%, common values for electrothermal vaporization used for sample introduction. No comparison was made related to dispersion of results obtained in laboratory and outside the location, since our instrumentation is not yet in portable version.

Table 2
Limits of detection of elements in SSETV-μCCP-OES compared to other analytical methods.

Element	λ (nm)	E_{ex} (eV)	E_{dissoc} (eV)	Limit of detection						
				SSETV-μCCP-OES (ng ml^{-1})[a]	SSETV-μCCP-OES (pg)[a]	μCCP-OES (ng ml^{-1})[b]	CCP-OES (ng ml^{-1})[c]	CCP-AFS (ng ml^{-1})	ICP-AES (ng ml^{-1})[g]	ETV-MPD-OES (pg)[h]
Ag	328.068	3.78	1.4	0.5	5	–	–		1.2	
Cd	228.802	5.41	3.8	1.5	15	85	65	4.3[d]		120
Cd	214.438		3.8						1.0	
Cu	324.754	3.82	4.9	5.6	56		25		1.5	130
Cu	510.554	3.82	4.9			590				
Pb	368.346	4.33	4.1	20	200					
Pb	405.781	4.38	4.1			735	125			650
Pb	220.351		4.1						35	
Pb	283.310		4.1					35[e]		
Zn	213.856	5.80	4.0	3.0	30	170	60	8.2[f]	0.4	20

[a] Calculated for 10 μl sample.
[b] Pneumatic nebulization without desolvation; 30 W plasma power; HR4000 microspectrometer, Ocean Optics [19].
[c] CCP torch with Mo tubular electrode and double ring electrode; 275 W plasma power; pneumatic nebulization without desolvation; high resolution spectrometer with photomultiplier tube detectors [34].
[d,e,f] Capacitively coupled plasma atomic fluorescence spectrometry; single tubular Mo electrode torch; 275 W plasma power; pneumatic nebulization without desolvation; HR4000 microspectrometer, Ocean Optics [32,35,36].
[g] Found in our laboratory using Spectro CIROS^{CCD} spectrometer; pneumatic nebulization without desolvation.
[h] Electrothermal vaporization optical emission spectrometry in Ar–H_2 microplasma; 4 W power level; 3 μl sample [31].

Table 3
Results (mg kg^{-1}) for the analysis of CRMs of soil and sediments.

	Ag		Cd		Cu		Pb		Zn	
	Found mean ± U[a]	Certified mean ± U	Found mean ± U[a]	Certified mean ± U	Found mean ± U[a]	Certified mean ± U	Found mean ± U[a]	Certified mean ± U	Found mean ± U[a]	Certified mean ± U
LGC6141	–	–	–	–	53.6 ± 12	51.1 ± 13	65.9 ± 14	75.8 ± 16	171 ± 14	169 ± 39
CRM 048-50G	78.0 ± 11.89	75.2 ± 1.57	142 ± 23.30	140 ± 3.28	258 ± 51.90	277 ± 6.03	84.5 ± 3.23	86.9 ± 2.42	701 ± 36.0	724 ± 21.2
BCR280R	–	–	0.78 ± 0.3	0.85 ± 0.1	51 ± 7	53 ± 6	–	–	225 ± 4	224 ± 25
LGC6135	–	–	–	–	106 ± 10	105 ± 5	391 ± 12	391 ± 16	316 ± 45	316 ± 41
CRM Material S1	–	–	0.3 ± 0.06	0.3 ± 0.08	–	–	17 ± 2.2	15 ± 3.6	39 ± 5.0	35 ± 3.3
CRM 025-050	114 ± 18.9	132 ± 82.6	376 ± 20.9	369 ± 46.3	7.83 ± 1.25	7.76 ± 1.68	1351 ± 126	1447 ± 203	51.8 ± 7.31	51.8 ± 8.29
BCR142R	–	–	0.310 ± 0.07	0.249 ± 0.01	67.1 ± 13.2	68.7 ± 1.3	25.1 ± 3.5	25.7 ± 1.6	95.8 ± 16.7	93.3 ± 2.7
NCSDC78301	–	–	2.74 ± 0.6	2.45 ± 0.3	59 ± 12	53 ± 6	74 ± 9	79 ± 12	265 ± 42	(251)[c]
Average recovery/%[b]	**95 ± 16**		**108 ± 18**		**101 ± 18**		**98 ± 10**		**102 ± 12**	
RSD[d]/ %	5.0–6.5		2.1–8.8		3.5–9.0		1.0–8.0		0.5–7.0	
t_{calc}[e]	1.013–4.098		0.369–3.750		0.241–2.151		0.738–3.912		0.615–3.442	

[a] U is expanded uncertainty for 95% confidence level (n=3 replicates).
[b] 95% confidence level.
[c] Indicative value.
[d] Relative standard deviation of repeatability (precision) for 5 successive measurements for each CRM sample.
[e] Calculated as $t=(|c-\mu|/s)\sqrt{n}$ where: c is the mean found content; μ is the mean certified content; s is the standard deviation for 3 replicate measurements.

4. Conclusions

A SSETV–μCCP-OES laboratory system was characterized in terms of emission spectrum and analytical capability for the simultaneous determination of several volatile elements in liquid samples after electrothermal vaporization from Rh coil filament. The analytical system was optimized regarding electrothermal vaporization of sample, plasma operation and recording of three-dimensional spectral episodes in order to achieve the simultaneous determination of Ag, Cd, Cu, Pb and Zn. The emission spectrum of elements was quite simple, dominated by the resonance lines, which allowed the use of a 0.4 nm-FWHM microspectrometer. The SSETV–μCCP-OES analytical system is useful for the determination of elements with excitation energy of atoms below 7 eV from microliter volumes with detection limits in the ng ml^{-1} or pg range. The analytical method based on SSETV–μCCP-OES was found to be affected by non-spectral interference of alkali and earth-alkaline elements, which required the use of the standard addition method for the analysis of soil and sediment samples with complex matrix. The usefulness of the analytical system for the simultaneous determination of elements was demonstrated by the analysis of soil and sediment CRMs with appropriate sensitivity, precision and accuracy. The analytical set-up is attractive due to simple construction of both electrothermal vaporization device and plasma microtorch, inexpensive following low power and low Ar consumption and easy-to-run in the multielemental analysis of liquid samples.

Acknowledgments

This work was supported by a Grant of the Romanian National Authority for Scientific Research, CNDI–UEFISCDI, Project number PN-II-PT-PCCA-2011-3.2-0219 (Contract no. 176/2012).

Appendix A. Supplementary information

Supplementary data associated with this article can be found in the online version at http://dx.doi.org/10.1016/j.talanta.2014.04.032.

References

[1] V. Karanassios, Spectrochim. Acta B 59B (2004) 909–926.
[2] M. Miclea, J. Franzke, Plasma Chem. Plasma Process. 27 (2007) 205–224.
[3] J.A.C. Broekaert, Appl. Spectrosc. 62 (2008) 227A–234A.
[4] X. Yuan, J. Tang, Y. Duan, Appl. Spectrosc. Rev. 46 (2011) 581–605.
[5] M. Puanngam, S.I. Ohira, F. Unob, J.H. Wang, P.K. Dasgupta, Talanta 81 (2010) 1109–1115.
[6] I.J. Zapata, P. Pohl, N.H. Bings, J.A.C. Broekaert, Anal. Bioanal. Chem. 388 (2007) 1615–1623.
[7] V. Cerveny, M. Horvath, J.A.C. Broekaert, Microchem. J. 107 (2013) 10–16.
[8] P. Jamroz, P. Pohl, W. Zyrnicki, J. Anal. At. Spectrom. 27 (2012) 1772–1779.
[9] T. Frentiu, A.I. Mihaltan, M. Ponta, E. Darvasi, M. Frentiu, E. Cordos, J. Hazard. Mater. 193 (2011) 65–69.
[10] X. Yuan, G. Yang, Y. Ding, X. Li, X. Zhan, Z. Zhao, Y. Duan, Spectrochim. Acta 93B (2014) 1–7.
[11] T. Frentiu, A.I. Mihaltan, E. Darvasi, M. Ponta, C. Roman, M. Frentiu, J. Anal. At. Spectrom. 27 (2012) 1753–1760.
[12] T. Frentiu, A.I. Mihaltan, M. Senila, E. Darvasi, M. Ponta, M. Frentiu, B. P. Pintican, Microchem. J. 110 (2013) 545–552.
[13] A.I. Mihaltan, T. Frentiu, M. Ponta, D. Petreus, M. Frentiu, E. Darvasi, C. Marutoiu, Talanta 109 (2013) 84–90.
[14] T. Frentiu, B.P. Pintican, S. Butaciu, A.I. Mihaltan, M. Ponta, M. Frentiu, Chem. Cent. J. 7 (2013) (paper 178).
[15] A. Kadenkin, J.A.C. Broekaert, J. Anal. At. Spectrom. 26 (2011) 1481–1487.
[16] T. Cserfalvi, P. Mezei, J. Anal. At. Spectrom. 9 (1994) 345–349.
[17] K. Greda, P. Jamroz, P. Pohl, Talanta 108 (2013) 74–82.
[18] Q. He, Z. Zhu, S. Hu, Appl. Spectrosc. Rev. 49 (2014) 249–269.
[19] T. Frentiu, D. Petreus, M. Senila, A.I. Mihaltan, E. Darvasi, M. Ponta, E. Plaian, E. Cordos, Microchem. J. (2011)188–195.
[20] A.R. Zsigmond, T. Frentiu, M. Ponta, M. Frentiu, D. Petreus, Food Chem. 141 (2013) 3621–3626.
[21] M Williams, E.H. Piepmeier, Anal. Chem. 44 (1972) 1342–1344.
[22] S.N. Hanna, B.T. Jones, Appl. Spectrosc. Rev. 46 (2011) 624–635.
[23] Z. Long, Y. Luo, C. Zheng, P. Deng, X. Hou, Appl. Spectrosc. Rev. 47 (2012) 382–413.
[24] I. Kula, Y. Arslan, S. Bakirdere, S. Titretir, E. Kenduzler, O.Y. Ataman, Talanta 80 (2009) 127–132.
[25] O. Alp, N. Ertas, Talanta 81 (2010) 516–520.
[26] H.R. Badiei, B. Lai, V. Karanassios, Spectrochim. Acta B 77B (2012) 19–30.
[27] H.R. Badiei, J. McEnaney, V. Karanassios, Spectrochim. Acta B 78B (2012) 42–49.
[28] H.R. Badiei, C. Liu, V. Karanassios, Microchem. J. 108 (2013) 131–136.
[29] V. Karanassios, K. Johnson, A.T. Smith, Anal. Bioanal. Chem. 388 (2007) 1595–1604.
[30] S. Weagant, V. Karanassios, Anal. Bioanal. Chem. 395 (2009) 577–589.
[31] S. Weagant, V. Chen, V. Karanassios, Anal. Bioanal. Chem. 401 (2011) 2865–2880.
[32] T. Frentiu, E. Darvasi, M. Senila, M. Ponta, E. Cordos, Talanta 76 (2008) 1170–1176.
[33] P.W.J.M. Boumans, Spectrochim. Acta 46B (1991) 431–445.
[34] E. Cordos, T. Frentiu, A.M. Rusu, S.D. Anghel, M. Ponta, Talanta 48 (1999) 827–837.
[35] T. Frentiu, M. Ponta, A.I. Mihaltan, E. Darvasi, M. Frentiu, E. Cordos, J. Anal. At. Spectrom. 25 (2010) 739–742.
[36] T. Frentiu, M. Ponta, A.I. Mihaltan, E. Darvasi, M. Frentiu, E. Cordos, Spectrochim. Acta 65B (2010) 565–570.